The Journal of Chemical Physics ARTICLE scitation.org/journal/jcp

Simplified tuning of long-range corrected density functionals for use in symmetry-adapted perturbation theory

Cite as: J. Chem. Phys. 155, 034103 (2021); doi: 10.1063/5.0059364
Submitted: 8 June 2021 • Accepted: 28 June 2021 •
Published Online: 15 July 2021

Montgomery Gray and John M. Herbert[a)]

AFFILIATIONS

Department of Chemistry and Biochemistry, The Ohio State University, Columbus, Ohio 43210, USA

[a)]Author to whom correspondence should be addressed: herbert@chemistry.ohio-state.edu

ABSTRACT

Long considered a failure, second-order symmetry-adapted perturbation theory (SAPT) based on Kohn–Sham orbitals, or SAPT0(KS), can be resurrected for semiquantitative purposes using long-range corrected density functionals whose asymptotic behavior is adjusted separately for each monomer. As in other contexts, correct asymptotic behavior can be enforced via "optimal tuning" based on the ionization energy theorem of density functional theory, but the tuning procedure is tedious, expensive for large systems, and comes with a troubling dependence on system size. Here, we show that essentially identical results are obtained using a fast, convenient, and automated tuning procedure based on the size of the exchange hole. In conjunction with "extended" (X)SAPT methods that improve the description of dispersion, this procedure achieves benchmark-quality interaction energies, along with the usual SAPT energy decomposition, without the hassle of system-specific tuning.

I. INTRODUCTION

Symmetry-adapted perturbation theory (SAPT) is the foremost *ab initio* theory of intermolecular interactions.[1–5] It provides a physically meaningful energy decomposition analysis (EDA) for intermolecular interactions, yet one that is capable of benchmark-quality interaction energies if extended to sufficiently high order. The lowest-order variant, known as "SAPT0,"[5,6] uses Hartree–Fock wave functions for the monomers in conjunction with second-order perturbation theory to describe the intermolecular interactions. Combined with appropriate basis sets, SAPT0 provides a semiquantitative treatment of noncovalent interactions at $\mathcal{O}(N^5)$ computational cost.[6] The description of strong hydrogen bonds can be improved through the use of Kohn–Sham orbitals from density functional theory (DFT), albeit at the expense of (further) degrading the description of dispersion,[7,8] which is already the least accurate component of SAPT0.[6–8] For this reason, the "SAPT0(KS)" approach, meaning SAPT0 with Kohn–Sham orbitals, was considered and rejected a long time ago.[9–13] The method can be salvaged, however, through the use of exchange-correlation functionals with correct asymptotic behavior.[8,14]

Benchmark-quality interaction energies can be achieved using alternative combinations of DFT with SAPT that replace second-order dispersion with a more accurate formulation. Of these alternatives, the most widely used is DFT-SAPT,[3,15] also known as SAPT(DFT),[2,16] which employs frequency-dependent density susceptibilities for the monomers (computed using DFT) to obtain the dispersion energy. In conjunction with density fitting techniques, DFT-SAPT is an $\mathcal{O}(N^5)$ method,[15,17] albeit one with a much larger prefactor as compared to SAPT0. Less costly alternatives include *ab initio* dispersion potentials[18–22] (SAPT+*ai*D) or the many-body dispersion method[23,24] (SAPT+MBD), which also avoid second-order dispersion. Both of the latter methods achieve accuracies of $\lesssim 1$ kcal/mol for benchmark noncovalent problems,[21–23] with $\mathcal{O}(N^3)$ scaling.[22] All of these DFT-based SAPT methods require the use of density functionals that are asymptotically correct. What that entails is described in Sec. II, and a convenient means to achieve this behavior is the topic of the present work.

II. THEORY

The asymptotic behavior of the exchange-correlation (xc) potential ought to be

$$v_{xc}(r) \sim v_{xc}(\infty) - \frac{1}{r} \tag{1}$$

for large r. The limiting value as $r \to \infty$ is

$$v_{xc}(\infty) = \mathrm{IE} + \varepsilon_{\mathrm{HOMO}}, \tag{2}$$

where $\mathrm{IE} = E(N-1) - E(N)$ is the ionization energy and $\varepsilon_{\mathrm{HOMO}}$ is the energy level of the highest-occupied molecular orbital (HOMO).[25] In the context of DFT-SAPT, correct asymptotic behavior has generally been grafted onto a standard semilocal approximation for v_{xc},[25–27] whereas in SAPT0(KS) it has usually been achieved using long-range corrected (LRC) density functionals.[8,14] The correct asymptotic shape, i.e., the condition $v_{xc}(r) \sim -1/r$, is achieved automatically if the exchange functional is 100% Hartree–Fock exchange in the limit $r \to \infty$. We use the term LRC-DFT to indicate the subset of range-separated hybrid functionals that satisfy this asymptotic condition.[28–33]

The use of LRC-DFT does not guarantee that the asymptotic value $v_{xc}(\infty)$ is correct, but this can be set by adjusting the range-separation parameter ω such that $\mathrm{IE}(\omega) = -\varepsilon_{\mathrm{HOMO}}(\omega)$, according to the ionization energy theorem in DFT.[34,35] In the context of time-dependent (TD-)DFT, this procedure has come to be called "optimal tuning"[33] and is widely used to correct the behavior of TD-DFT for charge-transfer excitations.[33–36] The same tuning procedure has been used for SAPT0(KS) calculations,[8,14,18–22] and we denote the range-separation parameter that satisfies the IE criterion as ω_{IE},

$$\mathrm{IE}(\omega_{\mathrm{IE}}) = -\varepsilon_{\mathrm{HOMO}}(\omega_{\mathrm{IE}}). \tag{3}$$

Although widely used, this "optimal" or IE-tuning procedure has two significant problems, one practical and the other fundamental. Fundamentally, it is problematic in small-gap systems, as demonstrated by the results presented herein. This is a more serious limitation than one might at first imagine because semilocal functionals tend (anomalously) toward vanishing gaps for large systems.[37–42] More pragmatically, the procedure is time-consuming and therefore acts as a deterrent to potential users of SAPT0(KS) and related methods.

In the present work, we explore the use of a black-box alternative to set ω based on the size of the exchange hole, in what has been called "global density-dependent" (GDD) tuning.[43] Here, the range-separation parameter is set to a value

$$\omega_{\mathrm{GDD}} = C\langle d_x^2 \rangle^{-1/2}, \tag{4}$$

in which d_x^2 is the second moment of the distance to the center of the exchange hole[44] and $\langle d_x^2 \rangle$ is a weighted average,

$$\langle d_x^2 \rangle = \frac{\int \rho(\mathbf{r})\, w(\mathbf{r})\, d_x^2(\mathbf{r})\, d\mathbf{r}}{\int \rho(\mathbf{r})\, w(\mathbf{r})\, d\mathbf{r}}. \tag{5}$$

The weighting function,[43]

$$w(\mathbf{r}) = \begin{cases} 1, & t(\mathbf{r}) \le \mu \\ 0, & t(\mathbf{r}) > \mu, \end{cases} \tag{6}$$

is itself defined in terms of function

$$t(\mathbf{r}) = \frac{\tau_{\mathrm{UEG}}(\mathbf{r})}{\tau(\mathbf{r})}, \tag{7}$$

where $\tau(\mathbf{r})$ is the kinetic energy density and $\tau_{\mathrm{UEG}}(\mathbf{r}) = 3(6\pi^2)^{2/3}\rho(\mathbf{r})^{5/3}/5$ is its value for the uniform electron gas. The orbital localization function $t(\mathbf{r})$ was originally introduced by Becke,[45,46] who used it to construct both the electron localization function[45] and the "localized orbital locator."[46] In the present context, $t(\mathbf{r})$ furnishes a weighting function that makes $w(\mathbf{r}) \approx 0$ in the region of localized orbitals so that ω_{GDD} is set based on asymptotics.[43] The parameter μ in Eq. (6) is determined self-consistently such that the denominator in Eq. (5) equals unity. Finally, C in Eq. (4) is an empirical parameter that is fit to reproduce the IE tuning condition in Eq. (3) for a set of small molecules.[22,43,47]

Both $w(\mathbf{r})$ and $d_x^2(\mathbf{r})$ are functionals of $\rho(\mathbf{r})$. As described in Ref. 43, the procedure is to first perform a self-consistent LRC-DFT calculation, e.g., using LRC-ωPBE with $\omega = 0.3\mathrm{bohr}^{-1}$. (This is an empirically optimized "best guess" for the range-separation parameter.[29–31]) The self-consistent density thus obtained is then used to evaluate ω_{GDD} in Eq. (4). The results are found to be negligibly different from a fully self-consistent procedure.[43] In the context of SAPT0(KS), the GDD tuning method obviates the need to perform IE tuning separately for each monomer. Some isolated comparisons of IE- vs GDD tuning for SAPT calculations were reported in Ref. 22, but here we report systematic comparisons for standard benchmark datasets of supramolecular complexes.

III. COMPUTATIONAL METHODS

We use the term SAPT0(KS) to refer to the second-order method that is generally called SAPT0 when it is based upon Hartree–Fock (HF) wave functions for the monomers.[5,6] For consistency, the traditional HF-based approach is labeled as SAPT0(HF) herein and is compared alongside methods such as SAPT0(B3LYP) and SAPT0(LRC-ωPBE) that use different self-consistent field (SCF) methods to obtain the orbitals. Note that SAPT0(KS) is distinct from DFT-SAPT,[3,15] which is also known as SAPT(DFT).[2,16]

We will also test "extended" (X)SAPT methods,[20–22] in which the SCF monomer wave functions are computed via the charge-embedded "XPol" procedure.[7,48,49] In the XSAPT calculations presented herein, the second-order dispersion energy

$$E_{\mathrm{disp}} = E_{\mathrm{disp}}^{(2)} + E_{\mathrm{exch-disp}}^{(2)} \tag{8}$$

is replaced by either atom–atom dispersion potentials fitted to *ab initio* dispersion data (XSAPT+*ai*D3)[21] or else a version of the many-body dispersion (MBD) model,[50,51] XSAPT+MBD.[23,24] The XSAPT calculations reported here use CM5 embedding charges.[24]

For the underlying LRC-DFT functional, we use LRC-ωPBE[30] unless stated otherwise. (Some calculations with LRC-μBOP[29,32] are reported in the supplementary material.) The parameter $C = 0.885$ in Eq. (4) was determined in previous work,[22] following Ref. 43 and using the same test set of small molecules. The best-fit value of C varies significantly with the fraction of short-range Hartree–Fock exchange but is only weakly sensitive to the basis set.[47] Values $C \approx 0.9$ are appropriate when the self-consistent LRC-ωPBE calculation is performed using $\omega = 0.3\mathrm{bohr}^{-1}$,[22,43] which is used here. Values of ω_{IE} and ω_{GDD} obtained for each monomer in each of

the systems considered here can be found in the supplementary material.

All calculations were performed using Q-Chem,[52] v. 5.3. For XSAPT calculations, we use the Karlsruhe "def2" basis sets,[53,54] whose convergence will be systematically tested. For SAPT0(KS) calculations, we use the jun-cc-pVDZ basis set,[55] which is a partially augmented version of cc-pVDZ.[56] This is a compromise choice that affords reasonable error cancellation in the second-order dispersion term.[6] Some SAPT0(KS) results using aug-cc-pVTZ[56,57] are reported in the supplementary material.

IV. RESULTS AND DISCUSSION

A. IE tuning for small-gap systems

We first demonstrate a looming problem with the IE-based tuning procedure for small-gap systems, using a homologous sequence of linear acenes: benzene, naphthalene, anthracene, tetracene, etc. As the number of rings increases, the Kohn–Sham gap for these one-dimensional nanoribbons decreases much faster than that of their saturated (cyclohexane-based) analogs, the perhydroacenes.[58]

Figure 1 compares tuned values ω_{IE} and ω_{GDD} obtained for acenes with up to 40 rings, demonstrating that both tuning procedures predict an optimal value of ω that decreases monotonically with system size. In the context of IE tuning, similar trends with increasing system size have been noted previously for conjugated π systems,[43,59–61] for linear alkanes,[43] for pentacene/C_{60} clusters,[62] and for $(H_2O)_n^-$ clusters.[63] In the present data, we note that the asymptotic value of ω_{GDD} is much larger than the asymptotic value of ω_{IE}. For the 40-ring acene, we obtain $\omega_{IE} = 0.046\,\text{bohr}^{-1}$, corresponding to a functional in which full HF exchange is activated on a length scale of $\sim 1/\omega_{IE} = 22$ bohrs. While this is much shorter than the length of the 40-acene ribbon, it is much longer than the length scale of a chemical bond, so from the standpoint of the dynamical correlation that contributes to thermochemistry, the LRC functional in question is operationally semilocal. In contrast, the GDD procedure converges to $\omega_{GDD} \approx 0.20\,\text{bohr}^{-1}$ for the longest nanoribbon,

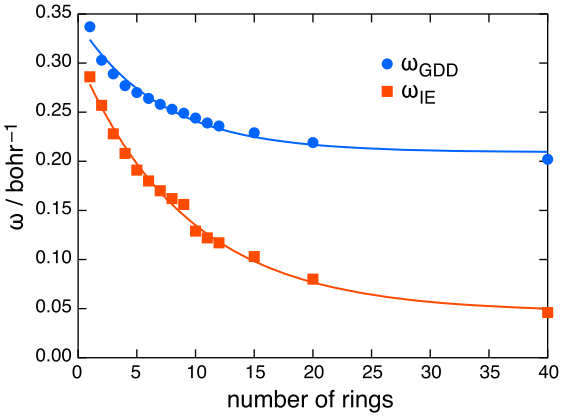

FIG. 1. Tuned values of ω for the linear acenes (benzene, naphthalene, anthracene, etc.), computed at the LRC-ωPBE/def2-TZVP level of theory. The results for LRC-μBOP are similar (see Fig. S1).

which is within the range of statistically optimized values of ω for LRC functionals.[29–31]

Note also what appears to be a small discontinuity in the progression of ω_{IE} values between nonacene and decacene, such that the data for $n < 10$ rings appear to extrapolate to a smaller asymptotic value of ω_{IE} as compared to the data for $n \geq 10$. This discontinuity appears also (at the same system size) when LRC-μBOP is used instead of LRC-ωPBE (see Fig. S1). This small jump may be related to the emergence of an open-shell singlet biradicaloid ground state of the linear acenes as the number of rings increases.[64,65] In any case, in combination with the vanishing of the HOMO/LUMO gap for large systems described by semilocal functionals,[37–42] these data present compelling evidence of an imminent problem with the IE tuning procedure as system size increases.

B. Evaluation of SAPT0(KS) methods

As a baseline and starting point for further discussion, Table I reports error statistics for the S66 dataset of small dimers,[66] obtained

TABLE I. Error statistics (in kcal/mol) for SAPT0(KS) methods applied to the S66 database and three subsets thereof.

	H-bonded		Disp.-bound		Mixed		All S66	
Method[a]	MAE[b]	Max[c]	MAE[b]	Max[c]	MAE[b]	Max[c]	MAE[b]	Max[c]
SAPT0(HF)	2.20	6.14	0.95	1.93	0.78	1.77	1.33	6.14
SAPT0(HF)+δHF	0.35	0.85	0.64	1.54	0.40	1.41	0.48	1.54
SAPT0(B3LYP)	1.49	4.24	1.49	3.93	0.66	1.36	1.24	4.24
SAPT0(B3LYP)+δHF	0.64	2.14	1.74	4.51	0.78	1.73	1.07	4.51
SAPT0(LRC-ωPBE)[d]	2.87	7.69	0.91	2.04	0.71	3.60	1.53	7.69
SAPT0(LRC-ωPBE)[d]+δHF	0.97	2.27	0.95	2.04	0.50	2.66	0.82	2.66
XSAPT[d]+*ai*D3	2.01	5.76	0.15	0.54	0.25	0.64	0.83	5.76
XSAPT[d]+*ai*D3+δHF	0.19	0.42	0.42	1.05	0.50	1.04	0.36	1.05
XSAPT[d]+MBD	2.00	5.76	0.15	0.54	0.25	0.64	0.83	5.76
XSAPT[d]+MBD+δHF	0.18	0.75	0.46	1.11	0.53	1.07	0.39	1.11

[a]The basis set is jun-cc-pVDZ for SAPT0(KS) and def2-TZVPPD for XSAPT.
[b]Mean absolute error, with respect to complete-basis CCSD(T) benchmarks from Ref. 66.
[c]Maximum absolute deviation with respect to the benchmarks.
[d]Uses LRC-ωPBE with ω_{GDD} tuning.

using a variety of SAPT0(KS) methods. (Additional error statistics, including percentage errors, can be found in Table S5.) The results are tabulated both with and without a "δHF" correction,[5,21]

$$\delta\mathrm{HF} = E_{\mathrm{int}}^{\mathrm{HF}} - \left(E_{\mathrm{elst}}^{(1)} + E_{\mathrm{exch}}^{(1)} + E_{\mathrm{ind,\,resp}}^{(2)} + E_{\mathrm{exch-ind,\,resp}}^{(2)}\right). \quad (9)$$

This correction consists of a counterpoise-corrected dimer HF calculation (to obtain $E_{\mathrm{int}}^{\mathrm{HF}}$), from which the non-dispersion parts of the second-order SAPT0(HF) interaction energy are subtracted. The result is an approximate correction for infinite-order induction. Note that the correction in Eq. (9) should use HF theory even for SAPT0(KS) methods based on DFT because only in the HF case can this correction be strictly classified as induction. A supramolecular DFT calculation mixes together different energy components in a manner that is difficult to separate.

Error statistics in Table I are separated into three subsets of S66: hydrogen-bonded dimers, dispersion-dominated dimers, and dimers where the interactions are mixed. This classification is based upon benchmark values of the electrostatic energy (E_{elst}) and the dispersion energy (E_{disp}).[66] The hydrogen-bonded subset consists of dimers for which $|E_{\mathrm{elst}}| \geq 2|E_{\mathrm{disp}}|$, which includes dimers composed of water, methanol, methylamine, and acetic acid. The dispersion-dominated complexes are characterized by $|E_{\mathrm{disp}}| \geq 2|E_{\mathrm{elst}}|$, which includes dimers drawn from benzene, pyridine, ethene, ethyne, and some larger hydrocarbons. Other dimers such as benzene–ethyne, ethyne–water, and benzene–acetic acid are classified as "mixed," meaning that they do not satisfy either of the aforementioned criteria. There are 23 dimers categorized as hydrogen-bonded, 23 categorized as dispersion-dominated, and 20 classified as mixed.[66]

The SAPT0(HF) and SAPT0(HF)+δHF results in Table I establish a baseline for what can be accomplished at low cost with traditional second-order SAPT. We also consider SAPT0(B3LYP), which was the lone representative of SAPT in a side-by-side comparison of different EDAs.[67] Although SAPT0(B3LYP) does offer a modest reduction in errors for hydrogen-bonded complexes, as compared to SAPT0(HF), those gains are wiped out once the δHF correction is added to both methods. Furthermore, the incorrect asymptotic behavior of B3LYP increases the errors for the dispersion-bound complexes, relative to the traditional SAPT0(HF) approach. This is especially noticeable if one expands the basis set from jun-cc-pVDZ to aug-cc-pVTZ; see Tables S4 and S6 for a summary of SAPT0(KS) error statistics in the larger basis set. For the dispersion-bound subset of S66, SAPT0(B3LYP)/aug-cc-pVTZ exhibits mean absolute errors greater than 110% (Table S6), whereas the HF-based method is less strongly affected by this change.

Overall, the B3LYP-based approach is outperformed by SAPT0(HF)+δHF. Whereas the authors of Ref. 67 concluded that the "best" EDAs are those based on supramolecular DFT, this assessment is based on a skewed evaluation of SAPT methods that fails to consider SAPT0(HF)+δHF or any SAPT0(KS) approach with proper asymptotic behavior. While "best" is a highly subjective assessment, the separation of energy components is better defined in SAPT0(KS) as compared to supramolecular DFT.[68–70]

The larger errors for dispersion-dominated dimers are mostly mitigated by using tuned SAPT0(LRC-ωPBE), bringing them more in line with dispersion errors incurred by the traditional SAPT0(HF) approach. One may therefore conclude that it is the second-order treatment of dispersion, rather than anything related to the density functional approximation, that represents the primary source of error at the SAPT0(LRC-ωPBE)+δHF level. This confirms earlier results suggesting that ω-tuning can put SAPT0(KS) on par with SAPT0(HF),[8] so that the former is not nearly as problematic as early reports suggested.[9–13] That said, SAPT0(KS) does not appear to offer a significant advantage over the traditional HF-based approach, and in particular both require the δHF correction in order to achieve ~ 1 kcal/mol accuracy for hydrogen bonds.

To move beyond second-order dispersion within the confines of perturbation theory requires methods with triple excitations and $\mathcal{O}(N^7)$ scaling.[5,6] Alternatively, the perturbative treatment of dispersion can be supplanted altogether, which is the unifying concept that underlies both DFT-SAPT[2,3] and XSAPT.[20–23] Whereas DFT-SAPT exhibits $\mathcal{O}(N^5)$ scaling with a sizable prefactor,[15,17] XSAPT is cubic-scaling method whose cost resembles the monomer DFT cost.[18,22] The performance of two variants, XSAPT+*ai*D3 and XSAPT+MBD, is characterized for the S66 dataset in Table I. Without the δHF correction, these methods exhibit mean errors < 1 kcal/mol, but the performance for hydrogen-bonded systems is worse than that, with outliers approaching 6 kcal/mol. With the δHF correction, the maximum error for the hydrogen-bonded complexes is reduced below 1 kcal/mol. Both of these variants clearly outperform other low-cost SAPT methods, although SAPT0(KS)+δHF/jun-cc-pVDZ is surprisingly competitive. As will be seen below, that is an artifact of the small size of the S66 dimers, which suppresses the dispersion term.[22]

C. IE vs GDD tuning

The main purpose of this work is to provide a side-by-side comparison of ω_{IE}- and ω_{GDD}-based results. We select XSAPT+MBD+δHF to make this comparison because it affords the highest overall accuracy among the variants considered in Table I, despite its reduced computational scaling as compared to SAPT0(KS). Table II compares error statistics for S66 using either IE or GDD tuning in several different basis sets. Previous work has demonstrated that triple-ζ basis sets are required to converge the electrostatic interactions,[21] so it is not surprising to observe that the errors for hydrogen-bonded complexes decrease when the double-ζ basis is replaced by a triple-ζ one, but it is pleasing to see that this also decreases both mean and maximum errors for the dispersion-dominated dimers. This situation should be contrasted with the use of jun-cc-pVDZ for SAPT0 calculations, for which electrostatic interactions are not fully converged (cf. Tables S5 and S6). The choice of jun-cc-pVDZ is a compromise intended to avoid large errors in second-order dispersion as the basis set limit is approached, but such compromises are not required if second-order dispersion is avoided. The data in Table II also highlight the benefit of diffuse functions. In our experience, users frequently decline to employ diffuse functions, presumably for reasons of cost, but the concomitant sacrifice in accuracy is undeniable.

The key observation in the present work is the fact that errors incurred by GDD tuning are nearly identical to the IE-tuned results. On the basis of the S66 data, there would seem to be no reason to perform the more tedious IE tuning procedure, which is also rather expensive for the larger systems that are considered below. As a counterpoint, the *ansatz* for ω_{GDD} in Eq. (4) was fitted to

TABLE II. Error statistics for S66,[66] computed at the XSAPT+MBD+δHF level using the tuned LRC-ωPBE functional.

		Error (kcal/mol)							
		H-bonded		Disp.-bound		Mixed		All S66	
Tuning	Basis set	MAE[a]	Max[b]	MAE[a]	Max[b]	MAE[a]	Max[b]	MAE[a]	Max[b]
ω_{IE}	def2-SVPD	1.13	3.21	1.62	2.98	1.33	2.36	1.37	3.21
ω_{GDD}	def2-SVPD	1.07	3.35	1.67	3.16	1.37	2.48	1.37	3.35
ω_{IE}	def2-TZVP	0.71	2.13	0.55	1.43	0.80	1.31	0.68	2.13
ω_{GDD}	def2-TZVP	0.65	1.20	0.55	1.60	0.85	1.41	0.68	1.60
ω_{IE}	def2-TZVPP	0.94	2.78	0.43	1.31	0.67	1.22	0.69	2.78
ω_{GDD}	def2-TZVPP	0.89	2.43	0.47	1.48	0.75	1.32	0.70	2.43
ω_{IE}	def2-TZVPD	0.25	0.81	0.40	0.94	0.50	0.91	0.38	0.94
ω_{GDD}	def2-TZVPD	0.21	0.57	0.45	1.18	0.57	1.06	0.40	1.18
ω_{IE}	def2-TZVPPD	0.24	1.36	0.42	0.97	0.47	0.93	0.37	1.36
ω_{GDD}	def2-TZVPPD	0.18	0.75	0.46	1.11	0.53	1.07	0.39	1.11

[a]Mean absolute error, with respect to complete-basis CCSD(T) benchmarks from Ref. 66.
[b]Maximum absolute deviation.

reproduce ω_{IE} for small molecules, and the monomers that comprise the S66 dimers are quite small, with the largest being pyridine (C_5H_5N), uracil ($C_4H_4N_2O_2$), and pentane (C_5H_{12}). We next consider some larger systems.

The L7 dataset[71] consists of dispersion-bound complexes ranging in size from (guanine)$_3$ up to coronene dimer, $(C_{24}H_{12})_2$, and also circumcoronene ($C_{54}H_{18}$) partnered with either adenine or else a guanine–cytosine base pair. Because the induction energies are small for these systems, the δHF correction makes little difference ($\lesssim 0.5$ kcal/mol), and in the absence of this correction, no supramolecular calculations are required for XSAPT. Interaction energies for L7, computed at the XSAPT+MBD/def2-TZVPPD level, are reported in Table III and compared to the newest set of complete-basis CCSD(T) benchmarks.[72]

The maximum discrepancy between the ω_{IE}- and ω_{GDD}-based results is 0.7 kcal/mol, for the complex between circumcoronene and guanine–cytosine, although the difference between the two XSAPT calculations amounts to a mere 2% of the benchmark interaction energy ($E_{int} = -28.63$ kcal/mol). The final column of Table III lists the difference between ω_{IE}- and ω_{GDD}-based interaction energies as a percentage of the benchmark value, and these differences are each $\lesssim 3\%$ except for the most weakly bound complex, (guanine)$_3$, for which the difference is 5% of the benchmark. For comparison, both sets of XSAPT+MBD calculations for L7 exhibit a mean absolute error of 6% with respect to the benchmarks, so the difference between tuning schemes is smaller than the inherent accuracy of either method.

In terms of absolute accuracy, the maximum XSAPT+MBD errors are 3.6 kcal/mol (ω_{IE}) and 3.0 kcal/mol (ω_{GDD}), both for the phenylalanine trimer, while the mean absolute errors (MAEs) are 1.3 kcal/mol (ω_{IE}) and 1.0 kcal/mol (ω_{GDD}). To put these numbers in perspective, the MAE for SAPT0(HF)/jun-cc-pVDZ as applied to the L7 dataset is 4.8 kcal/mol and the maximum error is 10.3 kcal/mol.[22] As compared to the S66 results, this represents a stark divergence in the performance of SAPT0 relative to XSAPT, and it occurs due to the much larger dispersion energies for the L7 complexes. These complexes reveal the failure of second-order dispersion, especially for π–π interactions.[21,22]

As a final example, we consider a DNA intercalation complex with the antitumor drug ellipticine, which has become a standard benchmark problem.[22–24,72,73] Interaction energies computed

TABLE III. XSAPT+MBD/def2-TZVPPD interaction energies for the L7 dataset of large dispersion-bound dimers.

		E_{int} (kcal/mol)		
System[a]	Tuning	XSAPT	Error[b]	$\Delta E_{int}(\omega)$[c] (%)
$(cor)_2$	ω_{IE}	−20.11	0.82	2.3
	ω_{GDD}	−20.60	0.33	
(circor)···(Ade)	ω_{IE}	−16.01	0.90	2.5
	ω_{GDD}	−16.43	0.58	
(circor)···GC	ω_{IE}	−26.43	2.20	2.4
	ω_{GDD}	−27.13	1.50	
$(octadecane)_2$	ω_{IE}	−12.31	1.31	0.3
	ω_{GDD}	−12.35	1.35	
$(GC)_2$	ω_{IE}	−13.61	0.07	2.8
	ω_{GDD}	−13.99	0.45	
$(Gua)_3$	ω_{IE}	−2.08	0.00	4.9
	ω_{GDD}	−2.19	0.11	
$(Phe)_3$	ω_{IE}	−21.84	3.62	2.3
	ω_{GDD}	−22.42	3.05	
MAE[d]	ω_{IE}		1.28	2.5
	ω_{GDD}		1.04	
Std. dev.[e]	ω_{IE}		1.18	1.2
	ω_{GDD}		0.95	

[a]cor = coronene, circor = circumcoronene, Ade = adenine, GC = guanine:cytosine base pair, Gua = guanine, Phe = phenylalanine.
[b]$E_{int}^{CCSD(T)} - E_{int}^{XSAPT}$, using benchmarks from Ref. 72.
[c]Difference between ω_{IE} and ω_{GDD} versions of E_{int}^{XSAPT}, expressed as a percentage of $E_{int}^{CCSD(T)}$.
[d]Mean absolute error.
[e]Standard deviation.

TABLE IV. Interaction energies for ellipticine bound to double-stranded DNA, computed using XSAPT+MBD.

Tuning	Basis	E_{int} (kcal/mol) XSAPT	Error[a]
ω_{IE}	def2-SVPD	−54.22	15.62
ω_{GDD}	def2-SVPD	−54.07	15.47
ω_{IE}	def2-TZVP	−43.14	4.54
ω_{GDD}	def2-TZVP	−42.89	4.29
ω_{IE}	def2-TZVPP	−42.91	4.31
ω_{GDD}	def2-TZVPP	−42.62	4.02
ω_{IE}	def2-TZVPD	−40.64	2.04
ω_{GDD}	def2-TZVPD	−40.44	1.84

[a]With respect to a complete-basis CCSD(T) benchmark, $E_{int} = -38.6 \pm 2.2$ kcal/mol.[72]

at the XSAPT+MBD level are presented in Table IV, using several different basis sets and comparing ω_{IE} and ω_{GDD} versions in each case. The two tuning schemes never deviate from one another by more than 0.3 kcal/mol. In terms of accuracy, the errors are reduced as the quality of the basis set is improved, and these calculations once again highlight the important role of diffuse functions: The XSAPT+MBD/def2-TZVPD interaction energies lie just within the estimated uncertainties of the benchmark, $E_{int} = -38.6 \pm 2.2$ kcal/mol.[72] For comparison, the best-available supramolecular DFT results for this system are $E_{int} = -41.3$ kcal/mol (B97M-V/def2-TZVPPD) and $E_{int} = -43.7$ kcal/mol (ωB97M-V/def2-TZVPPD),[24] corresponding to errors of 2.7 and 5.1 kcal/mol, respectively. As compared to supramolecular DFT, XSAPT+MBD is therefore more accurate,[24] but also cheaper,[23] as no supersystem calculation is required.

V. CONCLUSIONS

In the context of SAPT0(KS) and XSAPT methods, we find that the GDD tuning scheme works equally well as compared to IE-based tuning, but sidesteps the series of monomer calculations that are required for the latter. The GDD approach also avoids the size-dependent tuning catastrophe that afflicts IE tuning for small-gap systems, making it more robust in addition to being more convenient. Differences in interaction energies, when using one tuning scheme vs the other, are small in comparison to the inherent accuracy of the SAPT0(KS) and XSAPT methods themselves. Given its ease of use, GDD tuning should replace IE tuning for (X)SAPT calculations based on Kohn–Sham DFT, and indeed, our group has mostly relied on the GDD scheme in recent work.[22–24,74]

This work also highlights (and reiterates[8]) the fact that SAPT0(KS) methods should be based on asymptotically correct functionals for best results. Methods such as SAPT0(B3LYP), held up as an exemplar of a SAPT-based EDA,[67] actually misrepresent the accuracy of low-cost SAPT approaches. Correct asymptotic behavior is easily (and automatically) enforced using LRC functionals in conjunction with the tuning schemes examined herein. In conjunction with alternatives to second-order dispersion such as XSAPT+MBD,[23,24] this affords a cubic-scaling method with ~ 1 kcal/mol accuracy for noncovalent interaction energies, in systems large and small.

SUPPLEMENTARY MATERIAL

See the supplementary material for additional error statistics and other data including tuned values of ω.

ACKNOWLEDGMENTS

This work was supported by the U.S. Department of Energy, Office of Basic Energy Sciences, Division of Chemical Sciences, Geosciences, and Biosciences, under Award No. DE-SC0008550. Calculations were performed at the Ohio Supercomputer Center under Project No. PAA-0003.[75] J.M.H. serves on the board of directors of Q-Chem, Inc.

DATA AVAILABILITY

The data that support the findings of this study are available from the corresponding author upon reasonable request.

REFERENCES

[1]K. Szalewicz, K. Patkowski, and B. Jeziorski, "Intermolecular interactions via perturbation theory: From diatoms to biomolecules," in *Intermolecular Forces and Clusters II*, Structure and Bonding Vol. 116, edited by D. J. Wales (Springer-Verlag, Berlin, 2005), pp. 43–117.
[2]K. Szalewicz, "Symmetry-adapted perturbation theory of intermolecular forces," Wiley Interdiscip. Rev.: Comput. Mol. Sci. **2**, 254–272 (2012).
[3]G. Jansen, "Symmetry-adapted perturbation theory based on density functional theory for noncovalent interactions," Wiley Interdiscip. Rev.: Comput. Mol. Sci. **4**, 127–144 (2014).
[4]K. Patkowski, "Recent developments in symmetry-adapted perturbation theory," Wiley Interdiscip. Rev.: Comput. Mol. Sci. **10**, e1452 (2020).
[5]E. G. Hohenstein and C. D. Sherrill, "Wavefunction methods for noncovalent interactions," Wiley Interdiscip. Rev.: Comput. Mol. Sci. **2**, 304–326 (2012).
[6]T. M. Parker, L. A. Burns, R. M. Parrish, A. G. Ryno, and C. D. Sherrill, "Levels of symmetry adapted perturbation theory (SAPT). I. Efficiency and performance for interaction energies," J. Chem. Phys. **140**, 094106 (2014).
[7]J. M. Herbert, L. D. Jacobson, K. U. Lao, and M. A. Rohrdanz, "Rapid computation of intermolecular interactions in molecular and ionic clusters: Self-consistent polarization plus symmetry-adapted perturbation theory," Phys. Chem. Chem. Phys. **14**, 7679–7699 (2012).
[8]K. U. Lao and J. M. Herbert, "Symmetry-adapted perturbation theory with Kohn-Sham orbitals using non-empirically tuned, long-range-corrected density functionals," J. Chem. Phys. **140**, 044108 (2014).
[9]H. L. Williams and C. F. Chabalowski, "Using Kohn-Sham orbitals in symmetry-adapted perturbation theory to investigate intermolecular interactions," J. Phys. Chem. A **105**, 646–659 (2001).
[10]G. Jansen and A. Hesselmann, "Comment on 'Using Kohn–Sham orbitals in symmetry-adapted perturbation theory to investigate intermolecular interactions'," J. Phys. Chem. A **105**, 11156–11157 (2001).
[11]A. J. Misquitta and K. Szalewicz, "Intermolecular forces from asymptotically corrected density functional description of monomers," Chem. Phys. Lett. **357**, 301–306 (2002).
[12]A. Heßelmann and G. Jansen, "First-order intermolecular interaction energies from Kohn-Sham orbitals," Chem. Phys. Lett. **357**, 464–470 (2002).
[13]A. Heßelmann and G. Jansen, "Intermolecular induction and exchange-induction energies from coupled-perturbed Kohn-Sham density functional theory," Chem. Phys. Lett. **362**, 319–325 (2002).
[14]M. Hapka, Ł. Rajchel, M. Modrzejewski, G. Chałasiński, and M. M. Szczęśniak, "Tuned range-separated hybrid functionals in the symmetry-adapted perturbation theory," J. Chem. Phys. **141**, 134120 (2014).

[15]A. Heßelmann, G. Jansen, and M. Schütz, "Density-functional theory symmetry-adapted intermolecular perturbation theory with density fitting: A new efficient method to study intermolecular interaction energies," J. Chem. Phys. **122**, 014103 (2005).
[16]A. J. Misquitta and K. Szalewicz, "Symmetry-adapted perturbation-theory calculations of intermolecular forces employing density-functional description of monomers," J. Chem. Phys. **122**, 214109 (2005).
[17]R. Bukowski, R. Podeszwa, and K. Szalewicz, "Efficient calculation of coupled Kohn–Sham dynamic susceptibility functions and dispersion energies with density fitting," Chem. Phys. Lett. **414**, 111–116 (2005).
[18]K. U. Lao and J. M. Herbert, "Accurate intermolecular interactions at dramatically reduced cost: XPol+SAPT with empirical dispersion," J. Phys. Chem. Lett. **3**, 3241–3248 (2012).
[19]K. U. Lao and J. M. Herbert, "An improved treatment of empirical dispersion and a many-body energy decomposition scheme for the explicit polarization plus symmetry-adapted perturbation theory (XSAPT) method," J. Chem. Phys. **139**, 034107 (2013); Erratum **140**, 119901 (2014).
[20]L. D. Jacobson, R. M. Richard, K. U. Lao, and J. M. Herbert, "Efficient monomer-based quantum chemistry methods for molecular and ionic clusters," Annu. Rep. Comput. Chem. **9**, 25–56 (2013).
[21]K. U. Lao and J. M. Herbert, "Accurate and efficient quantum chemistry calculations of noncovalent interactions in many-body systems: The XSAPT family of methods," J. Phys. Chem. A **119**, 235–253 (2015).
[22]K. U. Lao and J. M. Herbert, "Atomic orbital implementation of extended symmetry-adapted perturbation theory (XSAPT) and benchmark calculations for large supramolecular complexes," J. Chem. Theory Comput. **14**, 2955–2978 (2018).
[23]K. Carter-Fenk, K. U. Lao, K.-Y. Liu, and J. M. Herbert, "Accurate and efficient *ab initio* calculations for supramolecular complexes: Symmetry-adapted perturbation theory with many-body dispersion," J. Phys. Chem. Lett. **10**, 2706–2714 (2019).
[24]K.-Y. Liu, K. Carter-Fenk, and J. M. Herbert, "Self-consistent charge embedding at very low cost, with application to symmetry-adapted perturbation theory," J. Chem. Phys. **151**, 031102 (2019).
[25]D. J. Tozer and N. C. Handy, "Improving virtual Kohn–Sham orbitals and eigenvalues: Application to excitation energies and static polarizabilities," J. Chem. Phys. **109**, 10180–10189 (1998).
[26]R. van Leeuwen and E. J. Baerends, "Exchange-correlation potential with correct asymptotic behavior," Phys. Rev. A **49**, 2421–2431 (1994).
[27]M. Grüning, O. V. Gritsenko, S. J. A. van Gisbergen, and E. J. Baerends, "Shape corrections to exchange-correlation potentials by gradient-regulated seamless connection of model potentials for inner and outer region," J. Chem. Phys. **114**, 652–660 (2001).
[28]A. W. Lange, M. A. Rohrdanz, and J. M. Herbert, "Charge-transfer excited states in a π-stacked adenine dimer, as predicted using long-range-corrected time-dependent density functional theory," J. Phys. Chem. B **112**, 6304–6308 (2008); Erratum **112**, 7345 (2008).
[29]M. A. Rohrdanz and J. M. Herbert, "Simultaneous benchmarking of ground- and excited-state properties with long-range-corrected density functional theory," J. Chem. Phys. **129**, 034107 (2008).
[30]M. A. Rohrdanz, K. M. Martins, and J. M. Herbert, "A long-range-corrected density functional that performs well for both ground-state properties and time-dependent density functional theory excitation energies, including charge-transfer excited states," J. Chem. Phys. **130**, 054112 (2009).
[31]A. W. Lange and J. M. Herbert, "Both intra- and interstrand charge-transfer excited states in B-DNA are present at energies comparable to, or just above, the $^1\pi\pi^*$ excitonic bright states," J. Am. Chem. Soc. **131**, 3913–3922 (2009).
[32]R. M. Richard and J. M. Herbert, "Time-dependent density-functional description of the ^1L_a state in polycyclic aromatic hydrocarbons: Charge-transfer character in disguise?," J. Chem. Theory Comput. **7**, 1296–1306 (2011).
[33]B. Alam, A. F. Morrison, and J. M. Herbert, "Charge separation and charge transfer in the low-lying excited states of pentacene," J. Phys. Chem. C **124**, 24653–24666 (2020).
[34]T. Stein, L. Kronik, and R. Baer, "Reliable prediction of charge transfer excitations in molecular complexes using time-dependent density functional theory," J. Am. Chem. Soc. **131**, 2818–2820 (2009).
[35]R. Baer, E. Livshits, and U. Salzner, "Tuned range-separated hybrids in density functional theory," Annu. Rev. Phys. Chem. **61**, 85–109 (2010).
[36]S. Kümmel, "Charge-transfer excitations: A challenge for time-dependent density functional theory that has been met," Adv. Energy Mater. **7**, 1700440 (2017).
[37]J. Antony and S. Grimme, "Fully *ab initio* protein-ligand interaction energies with dispersion corrected density functional theory," J. Comput. Chem. **33**, 1730–1739 (2012).
[38]E. Rudberg, "Difficulties in applying pure Kohn–Sham density functional theory electronic structure methods to protein molecules," J. Phys.: Condens. Matter **24**, 072202 (2012).
[39]H. J. Kulik, N. Luehr, I. S. Ufimtsev, and T. J. Martinez, "Ab initio quantum chemistry for protein structures," J. Phys. Chem. B **116**, 12501–12509 (2012).
[40]C. M. Isborn, B. D. Mar, B. F. E. Curchod, I. Tavernelli, and T. J. Martínez, "The charge transfer problem in density functional theory calculations of aqueously solvated molecules," J. Phys. Chem. B **117**, 12189–12201 (2013).
[41]G. Lever, D. J. Cole, N. D. M. Hine, P. D. Haynes, and M. C. Payne, "Electrostatic considerations affecting the calculated HOMO-LUMO gap in protein molecules," J. Phys.: Condens. Matter **25**, 152101 (2013).
[42]D. J. Cole and N. D. M. Hine, "Applications of large-scale density functional theory in biology," J. Phys.: Condens. Matter **28**, 393001 (2016).
[43]M. Modrzejewski, Ł. Rajchel, G. Chalasinski, and M. M. Szczesniak, "Density-dependent onset of the long-range exchange: A key to donor–acceptor properties," J. Phys. Chem. A **117**, 11580–11586 (2013).
[44]A. D. Becke and E. R. Johnson, "Exchange-hole dipole moment and the dispersion interaction," J. Chem. Phys. **122**, 154104 (2005).
[45]A. D. Becke and K. E. Edgecombe, "A simple measure of electron localization in atomic and molecular systems," J. Chem. Phys. **92**, 5397–5403 (1990).
[46]H. L. Schmider and A. D. Becke, "Chemical content of the kinetic energy density," J. Mol. Struct.: THEOCHEM **527**, 51–61 (2000).
[47]K. Carter-Fenk, C. J. Mundy, and J. M. Herbert, "Natural charge-transfer analysis: Eliminating spurious charge-transfer states in time-dependent density functional theory via diabatization, with application to projection-based embedding," J. Chem. Theory Comput (published online) (2021).
[48]L. D. Jacobson and J. M. Herbert, "An efficient, fragment-based electronic structure method for molecular systems: Self-consistent polarization with perturbative two-body exchange and dispersion," J. Chem. Phys. **134**, 094118 (2011).
[49]J. Gao, D. G. Truhlar, Y. Wang, M. J. M. Mazack, P. Löffler, M. R. Provorse, and P. Rehak, "Explicit polarization: A quantum mechanical framework for developing next generation force fields," Acc. Chem. Res. **47**, 2837–2845 (2014).
[50]A. Tkatchenko, R. A. DiStasio, Jr., R. Car, and M. Scheffler, "Accurate and efficient method for many-body van der Waals interactions," Phys. Rev. Lett. **108**, 236402 (2012).
[51]A. Ambrosetti, A. M. Reilly, R. A. DiStasio, Jr., and A. Tkatchenko, "Long-range correlation energy calculated from coupled atomic response functions," J. Chem. Phys. **140**, 18A508 (2014).
[52]Y. Shao, Z. Gan, E. Epifanovsky, A. T. B. Gilbert, M. Wormit, J. Kussmann, A. W. Lange, A. Behn, J. Deng, X. Feng, D. Ghosh, M. Goldey, P. R. Horn, L. D. Jacobson, I. Kaliman, R. Z. Khaliullin, T. Kuś, A. Landau, J. Liu, E. I. Proynov, Y. M. Rhee, R. M. Richard, M. A. Rohrdanz, R. P. Steele, E. J. Sundstrom, H. L. Woodcock III, P. M. Zimmerman, D. Zuev, B. Albrecht, E. Alguire, B. Austin, G. J. O. Beran, Y. A. Bernard, E. Berquist, K. Brandhorst, K. B. Bravaya, S. T. Brown, D. Casanova, C.-M. Chang, Y. Chen, S. H. Chien, K. D. Closser, D. L. Crittenden, M. Diedenhofen, R. A. DiStasio, Jr., H. Do, A. D. Dutoi, R. G. Edgar, S. Fatehi, L. Fusti-Molnar, A. Ghysels, A. Golubeva-Zadorozhnaya, J. Gomes, M. W. D. Hanson-Heine, P. H. P. Harbach, A. W. Hauser, E. G. Hohenstein, Z. C. Holden, T.-C. Jagau, H. Ji, B. Kaduk, K. Khistyaev, J. Kim, J. Kim, R. A. King, P. Klunzinger, D. Kosenkov, T. Kowalczyk, C. M. Krauter, K. U. Lao, A. Laurent, K. V. Lawler, S. V. Levchenko, C. Y. Lin, F. Liu, E. Livshits, R. C. Lochan, A. Luenser, P. Manohar, S. F. Manzer, S.-P. Mao, N. Mardirossian, A. V. Marenich, S. A. Maurer, N. J. Mayhall, C. M. Oana, R. Olivares-Amaya, D. P. O'Neill, J. A. Parkhill, T. M. Perrine, R. Peverati, P. A. Pieniazek, A. Prociuk, D. R. Rehn, E. Rosta, N. J. Russ, N. Sergueev, S. M. Sharada, S. Sharma, D. W. Small, A. Sodt, T. Stein, D.

Stück, Y.-C. Su, A. J. W. Thom, T. Tsuchimochi, L. Vogt, O. Vydrov, T. Wang, M. A. Watson, J. Wenzel, A. White, C. F. Williams, V. Vanovschi, S. Yeganeh, S. R. Yost, Z.-Q. You, I. Y. Zhang, X. Zhang, Y. Zhao, B. R. Brooks, G. K. L. Chan, D. M. Chipman, C. J. Cramer, W. A. Goddard III, M. S. Gordon, W. J. Hehre, A. Klamt, H. F. Schaefer III, M. W. Schmidt, C. D. Sherrill, D. G. Truhlar, A. Warshel, X. Xu, A. Aspuru-Guzik, R. Baer, A. T. Bell, N. A. Besley, J.-D. Chai, A. Dreuw, B. D. Dunietz, T. R. Furlani, S. R. Gwaltney, C.-P. Hsu, Y. Jung, J. Kong, D. S. Lambrecht, W. Liang, C. Ochsenfeld, V. A. Rassolov, L. V. Slipchenko, J. E. Subotnik, T. Van Voorhis, J. M. Herbert, A. I. Krylov, P. M. W. Gill, and M. Head-Gordon, "Advances in molecular quantum chemistry contained in the Q-Chem 4 program package," Mol. Phys. **113**, 184–215 (2015).

[53]F. Weigend and R. Ahlrichs, "Balanced basis sets of split valence, triple zeta valence and quadruple zeta valence quality for H to Rn: Design and assessment of accuracy," Phys. Chem. Chem. Phys. **7**, 3297–3305 (2005).

[54]D. Rappoport and F. Furche, "Property-optimized Gaussian basis sets for molecular response calculations," J. Chem. Phys. **133**, 134105 (2010).

[55]E. Papajak, J. Zheng, X. Xu, H. R. Leverentz, and D. G. Truhlar, "Perspectives on basis sets beautiful: Seasonal plantings of diffuse basis functions," J. Chem. Theory Comput. **7**, 3027–3034 (2011).

[56]T. H. Dunning, Jr., "Gaussian basis sets for use in correlated molecular calculations. I. The atoms boron through neon and hydrogen," J. Chem. Phys. **90**, 1007–1023 (1989).

[57]R. A. Kendall, T. H. Dunning, Jr., and R. J. Harrison, "Electron affinities of the first-row atoms revisited. Systematic basis sets and wave functions," J. Chem. Phys. **96**, 6796–6806 (1992).

[58]K. Carter-Fenk and J. M. Herbert, "Reinterpreting π-stacking," Phys. Chem. Chem. Phys. **22**, 24870–24886 (2020).

[59]T. Körzdörfer, J. S. Sears, C. Sutton, and J.-L. Brédas, "Long-range corrected hybrid functionals for π-conjugated systems: Dependence of the range-separation parameter on conjugation length," J. Chem. Phys. **135**, 204107 (2011).

[60]T. B. de Queiroz and S. Kümmel, "Charge-transfer excitations in low-gap systems under the influence of solvation and conformational disorder: Exploring range-separation tuning," J. Chem. Phys. **141**, 084303 (2014).

[61]J. Bois and T. Körzdörfer, "Size-dependence of nonempirically tuned DFT starting points for G_0W_0 applied to π-conjugated molecular chains," J. Chem. Theory Comput. **13**, 4962–4971 (2017).

[62]B. Yang, Y. Yi, C.-R. Zhang, S. G. Aziz, V. Coropceanu, and J.-L. Brédas, "Impact of electron delocalization on the nature of the charge-transfer states in model pentacene/C_{60} interfaces: A density functional theory study," J. Phys. Chem. C **118**, 27648–27656 (2014).

[63]F. Uhlig, J. M. Herbert, M. P. Coons, and P. Jungwirth, "Optical spectroscopy of the bulk and interfacial hydrated electron from ab initio calculations," J. Phys. Chem. A **118**, 7507–7515 (2014).

[64]M. Bendikov, H. M. Duong, K. Starkey, K. N. Houk, E. A. Carter, and F. Wudl, "Oligoacenes: Theoretical prediction of open-shell singlet diradical ground states," J. Am. Chem. Soc. **126**, 7416–7417 (2004); Erratum **126**, 10493 (2004).

[65]Y. Yang, E. R. Davidson, and W. Yang, "Nature of ground and electronic excited states of higher acenes," Proc. Natl. Acad. Sci. U. S. A. **113**, E5098–E5107 (2016).

[66]J. Řezác, K. E. Riley, and P. Hobza, "S66: A well-balanced database of benchmark interaction energies relevant to biomolecular structures," J. Chem. Theory Comput. **7**, 2427–2438 (2011); Erratum **10**, 1359–1360 (2014).

[67]M. J. S. Phipps, T. Fox, C. S. Tautermann, and C.-K. Skylaris, "Energy decomposition analysis approaches and their evaluation on prototypical protein–drug interaction patterns," Chem. Soc. Rev. **44**, 3177–3211 (2015).

[68]K. U. Lao and J. M. Herbert, "Energy decomposition analysis with a stable charge-transfer term for interpreting intermolecular interactions," J. Chem. Theory Comput. **12**, 2569–2582 (2016).

[69]M. Shahbaz and K. Szalewicz, "Do semilocal density-functional approximations recover dispersion energies at small intermonomer separations?," Phys. Rev. Lett. **121**, 113402 (2018).

[70]J. Andrés, P. W. Ayers, R. A. Boto, R. Carbó-Dorca, H. Chermette, J. Cioslowski, J. Contreras-García, D. L. Cooper, G. Frenking, C. Gatti, F. Heidar-Zadeh, L. Joubert, Á. M. Pendás, E. Matito, I. Mayer, A. J. Misquitta, Y. Mo, J. Pilmé, P. L. A. Popelier, M. Rahm, E. Ramos-Cordoba, P. Salvador, W. H. E. Schwarz, S. Shahbazian, B. Silvi, M. Solà, K. Szalewicz, V. Tognetti, F. Weinhold, and É.-L. Zins, "Nine questions on energy decomposition analysis," J. Comput. Chem. **40**, 2248–2283 (2019).

[71]R. Sedlak, T. Janowski, M. Pitoňák, J. Řezáč, P. Pulay, and P. Hobza, "Accuracy of quantum chemical methods for large noncovalent complexes," J. Chem. Theory Comput. **9**, 3364–3374 (2013).

[72]F. Ballesteros, S. Dunivan, and K. U. Lao, "Coupled cluster benchmarks of large noncovalent complexes: The L7 dataset as well as DNA-ellipticine and buckycatcher-fullerene," J. Chem. Phys. **154**, 154104 (2021).

[73]A. Benali, L. Shulenburger, N. A. Romero, J. Kim, and O. A. von Lilienfeld, "Application of diffusion Monte Carlo to materials dominated by van der Waals interactions," J. Chem. Theory Comput. **10**, 3417–3422 (2014).

[74]K. U. Lao and J. M. Herbert, "A simple correction for nonadditive dispersion within extended symmetry-adapted perturbation theory (XSAPT)," J. Chem. Theory Comput. **14**, 5128–5142 (2018).

[75]Ohio Supercomputer Center, http://osc.edu/ark:/19495/f5s1ph73.